Journal of Sound and Vibration 325 (2009) 742–754

Contents lists available at ScienceDirect

Journal of Sound and Vibration

journal homepage: www.elsevier.com/locate/jsvi

Vibration reduction on beams subjected to moving loads using linear and nonlinear dynamic absorbers

Farhad S. Samani [a], Francesco Pellicano [b,*]

[a] Department of Mechanical Engineering, Bahonar University of Kerman, Kerman, Iran
[b] Department of Mechanical and Civil Engineering, University of Modena and Reggio Emilia, V. Vignolese, 905, 41100 Modena, Italy

ARTICLE INFO

Article history:
Received 22 September 2008
Received in revised form
7 April 2009
Accepted 8 April 2009
Handling Editor: A.V. Metrikine
Available online 17 May 2009

ABSTRACT

The present work is focused on the analysis of the effectiveness of dynamic vibration absorbers applied to beams excited by moving loads. The goal is to test the performance of nonlinear dampers in comparison with the classical linear damper. Simply supported beams are analysed using the Euler–Bernoulli theory, the partial differential equation governing the beam dynamics are reduced to an ordinary differential equation set by means of the Galerkin–Bubnov method, and a multimode expansion of the displacement field allows accurate analysis of the problem. The performance of the dynamic dampers in vibration reduction is estimated through two indicators, the maximum amplitude of vibration, and the portion of energy dissipated by the dynamic damper. The same indicators are used as objective functions for developing an optimisation approach. Two conservation laws are found for the optimal parameters and beam geometry for nonlinear (cubic) dynamic dampers.

1. Introduction

Studies on oscillations of bridges under travelling loads date back to the middle of the nineteenth century, when the early railways were developed; such applications are the most important examples of travelling loads. Readers interested in a comprehensive treatment of structures excited by moving loads are advised to read Ref. [1], which reports several applications.

One of the first modern studies on the subject of moving loads is due to Timoshenko et al. [2], who found an analytical solution to the problem, and derived an expression for the critical velocity. Considering moving masses instead of moving loads seems to be more realistic; however, in Ref. [3] it was shown that the behaviour of beams under moving loads or moving masses is very similar when the moving mass is assumed to be small in comparison to the beam mass.

The vibration of structures can be controlled by suitable structural design or by using active/passive devices, which are of particular interest when no modifications can be made to the structure. Primary qualities of passive devices include extremely low maintenance requirements and no need for supplied power.

A short analysis of the literature strictly related to the present work will now be presented. Wu [4] proposed the use of a linear dynamic absorber for beams subjected to moving loads, with the damper positioned in the middle of the beam span. The finite element method (FEM) was used to model the beam, and the dynamics were analysed after the governing equations were reduced to the first modal coordinate; i.e., the N-dof problem arising from the FEM was reduced to a 1-dof

* Corresponding author. Tel.: +39 0592056154; fax: +39 0592056126.
E-mail addresses: farhad.samani@yahoo.com (F.S. Samani), francesco.pellicano@unimore.it (F. Pellicano).

0022-460X/$ - see front matter © 2009 Elsevier Ltd. All rights reserved.
doi:10.1016/j.jsv.2009.04.011

model. This simplified model was used to obtain optimal values for the stiffness and damping ratio of the absorber, following Den Hartog's approach [5]. It should be mentioned that in the Wu model, the absorber equation was modified to take the spring mass into account.

Greco and Santini [6] analysed a beam under moving loads, with two rotational viscous dampers attached at its ends, and showed numerically that the effectiveness of the damper is strongly dependant on the speed of the moving load. Lee et al. [7] analysed the dynamics of a 2-dof system consisting of a grounded linear oscillator coupled to a light mass through an essentially nonlinear spring. They found that the periodic orbits of the undamped system greatly influence the damped dynamics, and presented evidence that complicated transitions between modes occur in the damped transient motion of this system.

Kwon et al. [8] proved that when a TGV train (Train a Grande Vitesse, French "high-speed train") passes a bridge, the maximum vertical displacement induced by the TGV is decreased by 21 percent and the free vibration dies more quickly when a tuned mass damper (TMD) is placed at the middle of the bridge. In Ref. [9], a new approach was presented for the reduction of the resonant vibration of simply supported beams under moving loads. In this treatment, viscous dampers were used to connect the main beam, which carries the loads, to an auxiliary beam placed underneath the main one. The results show that the resonant response of the main beam can be drastically reduced with this type of device.

The application of passive TMDs to suppress train-induced vibration on bridges was studied in Ref. [10]. It was shown that if the maximum dynamic response of the bridge and train are dominated by the resonant response within the design range of train speeds, a passive TMD performs well in vibration control.

Yau and Yang [11] studied vibration reduction for cable-stayed bridges subjected to the passage of high-speed trains. The train was modelled as a series of spring masses, the bridge deck and towers as nonlinear beam-column elements, and the stay cables as truss elements with Ernst's equivalent modulus. The numerical examples demonstrated that the proposed hybrid TMD system, which consisted of several dynamic dampers tuned to different dominant frequencies of the main structure, is effective for suppressing the multiple resonant vibration peaks encountered in cable-stayed bridges used by high-speed trains.

In Ref. [12], it was proved that TMDs tuned to a particular mode have a negligible effect on the other modes. The effectiveness of TMDs in reducing the vibration of primary structures subjected to random loads depends heavily upon the distribution of the eigenfrequencies.

In Ref. [13], Lin et al. studied an elastic beam subjected to a moving vehicle. They used a linear TMD as an energy-absorbing system, and presented results regarding the parameters of several absorbers. The roughness of the road was considered, with the assumption that the road profile could be modelled as a stationary random process. Lin [14] studied the use of a multi-time scale fuzzy controller for vibration reduction of an elastic continuum carrying a moving mass–spring–damper oscillator. This method is very effective for reducing the maximum deflection.

It was shown recently in Refs. [15–17] that under certain conditions, essentially nonlinear dynamic dampers can passively absorb energy from a linear non-conservative (damped) structure, acting as an essentially nonlinear energy sink (NES). Georgiades and Vakakis [15] provided numerical evidence of broadband passive targeted energy transfer from a linear flexible beam under shock excitation to a local NES. They showed numerically that an appropriately designed and placed NES can passively absorb and locally dissipate a significant fraction of the shock energy of the beam, up to an optimal value of 87 percent. The essential nonlinearity (nonlinearisable) of the attachment enables it to resonate with any of the linearised modes of the substructure, leading to the energy pumping phenomenon, i.e., passive, one-way, irreversible transfer of energy from the substructure to the attachment [16].

In the present work, the dynamics of an Euler–Bernoulli beam subjected to a moving load and coupled to a linear or essentially nonlinear (cubic) dynamic damper are studied. The goal is to find the optimal damper parameters (location, stiffness, and damping), and to compare the effectiveness of linear and nonlinear dampers. The goals of the optimisation are to minimise the absolute maximum deflection, or to maximise the amount of energy transferred from the beam to the damper. The temporal and spatial positions of the maximum beam deflection are unknown; therefore, a suitable search must be carried out. When the portion of the input energy dissipated by the dynamic damper is evaluated, it is crucial to correctly estimate the duration of the phenomenon.

The partial differential equations governing the beam dynamics have been reduced to a set of ordinary differential equations (ODEs) by means of the Galerkin–Bubnov approach, which leads to a linear or nonlinear system of ODEs, depending on the type of damper connected to the beam. Eigenfunctions of the beam problem without dampers are considered in the displacement expansion. Both linear and nonlinear models have been tested by comparison with the literature, and convergence tests have been performed in order to truncate the series without loss of accuracy.

The evaluation of the objective functions requires an accurate solution of the transient vibration of the system of ODEs. In order to use a general approach, the dynamics are studied by numerically integrating the ODEs using the Gauss–Kronrod method (Mathematica [18]), which is based on adaptive Gaussian quadrature with error estimation, through evaluation at Kronrod points.

Two optimisation strategies are used in this paper. The first is a brute force approach that consists of spanning the parameter space; such an approach suffers from a huge computational cost, and gives coarse results when the parameter space is large. The second approach is a random search, which consists of randomly selecting all parameters of interest, such method is slightly more efficient than the brute force approach, and more suitable for a large parameter space.

2. Dynamical system and basic equations

Consider the system represented in Fig. 1; a simply supported beam is connected to a small mass through a linear or nonlinear spring and a linear viscous damper, and the beam is loaded with a point load that can be either moving or time-varying. In this paper, "bare beam" means the beam without any attachment, see Ref. [4].

Using linear Euler–Bernoulli theory to model the beam, the equations of motion of the system are given by

$$EIy_{,xxxx}(x,t)+\rho Ay_{,tt}(x,t)+[f(u)+\lambda u_{,t}(t)]\delta(x-d)=F(x,t),\quad x\in(0,L),\ \ t>0 \tag{1a}$$

$$y(0,t)=0,\quad y(L,t)=0,\quad y_{,xx}(0,t)=0,\quad y_{,xx}(L,t)=0 \tag{1b}$$

$$y(x,0)=0,\quad y_{,t}(x,0)=0 \tag{1c}$$

$$m_0v_{,tt}(t)-f(u)-\lambda u_{,t}(t)=0,\quad v(0)=0,\ \ v_{,t}(0)=0,\ \ t>0 \tag{2a}$$

$$u(t)=y(d,t)-v(t),\quad f(u)=ku \text{ or } Cu^3 \tag{2b}$$

The beam dynamics are governed by the PDE represented by Eq. (1a), with simply supported boundary conditions (1b) and initial conditions (1c). The term $[f(u)+\lambda u_{,t}(t)]\delta(x-d)$ represents the force exerted by the dynamic damper, $f(u)$ is the stiffness force (see Eq. (2b) for definition), $\lambda u_{,t}(t)$ is the viscous damping force, and $\delta(x-d)$ defines the location of the dynamic damper. $F(x,t)$ is the external force, which can have time dependences in the amplitude (transient excitation) or the position along the beam (moving load). Eq. (2a) governs the dynamics of the dynamic damper, $y(x,t)$ is the transverse displacement field of the beam (down is positive), $y_{,x}=\partial y/\partial x$ (similar notation is used for other derivatives), E is the Young's modulus, I is the moment of inertia of the cross-sectional area, $m=\rho A$ is the mass per unit length, ρ is the material density, A is the cross-sectional area, $v(t)$ is the absolute position of the mass m_0, $x=d$ represents the location of the damper on the beam, λ is the damping coefficient of the viscous damper, and m_0 is the mass of the dynamic damper.

The attached mass is lightweight compared to the beam mass. Using a heavy dynamic damper gives more effective beam vibration reduction, however, the static deflection of the beam increases as well. Therefore, the mass of the absorber cannot be too large; in this work, the lumped mass of the absorber is taken to be 5 percent of the total mass of the beam [4].

The dynamics of the system represented by Eqs. (1) and (2) are analysed after projecting the partial differential Eq. (1a) into a complete, orthonormal basis. For the present problem, the eigenfunctions of the linear operator representing the simply supported beam with no attachments can be used.

$$\phi_r(x)=(2/mL)^{1/2}\sin(r\pi x/L),\quad \omega_r=(r\pi)^2(EI/mL^4)^{1/2},\ \ r=1,2,\ldots \tag{3a}$$

where ω_r is the natural frequency of the rth mode.

The eigenfunctions satisfy the following orthonormality conditions,

$$\int_0^L m\phi_i(x)\phi_j(x)\,\mathrm{d}x=\delta_{ij};\quad \int_0^L \phi_i(x)(EI\phi_j''(x))''\,\mathrm{d}x=\omega_j^2\delta_{ij},\ \ i,j=1,2,\ldots \tag{3b}$$

where δ_{ij} is Kronecker's delta and $(\cdot)'=\mathrm{d}(\cdot)/\mathrm{d}x$.

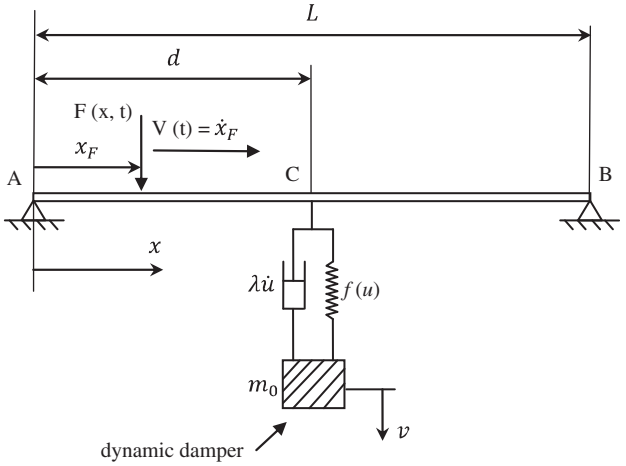

Fig. 1. The beam model.

It can be assumed that the transverse vibration of the beam is of the form

$$y(x,t)=\sum_{r=1}^{\infty}a_r(t)\phi_r(x) \tag{4}$$

where the $a_r(t)$ are unknown functions of time (modal coordinates) and the $\phi_r(x)$ are the normalised eigenfunctions.

By substituting Eq. (4) into Eqs. (1) and (2), projecting onto the pth eigenfunction, and using the orthonormality conditions, the following equations are obtained

$$\ddot{a}_p(t)+2\xi_p\omega_p\dot{a}_p(t)+\omega_p^2a_p(t)+\left\{D(t)+\lambda\left[\sum_{r=1}^{\infty}\dot{a}_r(t)\phi_r(d)-\dot{v}(t)\right]\right\}\phi_p(d)=\bar{F}(t),\quad p=1,2,\ldots \tag{5a}$$

$$m_0\ddot{v}(t)-D(t)+\lambda\left[\dot{v}(t)-\sum_{r=1}^{\infty}\dot{a}_r(t)\phi_r(d)\right]=0 \tag{5b}$$

where $\dot{a}_p(t)=\mathrm{d}a_p/\mathrm{d}t$ and

$$\begin{cases} D(t)=k\left[\sum\limits_{r=1}^{\infty}a_r(t)\phi_r(d)-v(t)\right] & \text{For linear dynamic damper} \quad (5c)\\ D(t)=C\left[\sum\limits_{r=1}^{\infty}a_r(t)\phi_r(d)-v(t)\right]^3 & \text{For nonlinear dynamic damper} \quad (5d)\end{cases}$$

$$\begin{cases} \bar{F}(t)=F_0\phi_p(Vt)\left[H\left(L/V-t\right)\right] & \text{For moving load} \quad (5e)\\ \bar{F}(t)=F_1(t)\phi_p(x_F) & \text{For transient constant load} \quad (5f)\end{cases}$$

which are obtained by considering the following forces in Eq. (1a)

$$\begin{cases} F(x,t)=F_0\delta(x-Vt)\left[H\left(\frac{L}{V}-t\right)\right] & \text{For moving load} \quad (6a)\\ F(x,t)=F_1(t)\delta(x-x_F) & \text{For transient constant load} \quad (6b)\end{cases}$$

where δ is the Dirac delta function, and $H(t)$ is the Heaviside function:

$$H(t)=\begin{cases}0, & t<0\\ 1, & t>0\end{cases} \tag{7}$$

A viscous damping term is added to the generic modal Eq. (5a) after projection.

The attachment couples to all modes through the infinite sum terms. In the case of a linear dynamic damper, one can transform system (5) by finding the new vibration modes; conversely, in the case of a nonlinear spring, the system cannot be decoupled.

The transient dynamics are studied by numerically integrating the dynamical system represented by Eqs. (5a) and (5b) after truncating series (4); the truncation is suitably chosen by checking the convergence of the expansion.

3. Validation

3.1. Nonlinear dynamic damper and fixed transient load

In order to check the accuracy of the present model, the case of a beam connected to a nonlinear dynamic damper and loaded with a transient force at a fixed position on the beam is now investigated, and compared with Ref. [15].

Consider the system of Fig. 1, with $V=0$, $x_F=$ constant, and $f(u)=Cu^3$. An impulsive force (a half sine pulse) excites the beam

$$F_1(t)=\begin{cases}F_a\sin(2\pi t/T), & 0\leqslant t<T/2\\ 0, & t<0 \text{ and } t\geqslant T/2\end{cases} \tag{8}$$

For comparison, the following parameters are considered: $F_a=10.0\,\mathrm{N}$, $T=(0.4/\pi)\mathrm{s}$, $EI=1.0\,\mathrm{Pa\,m^4}$, $\rho A=1.0\,\mathrm{kg/m}$, $2\xi_p\omega_p=0.05\,\mathrm{s^{-1}}$, $L=1.0\,\mathrm{m}$, $m_0=0.1\,\mathrm{kg}$, $x_F=0.3\,\mathrm{m}$, $\lambda=0.05\,\mathrm{N\,s/m}$, $d=0.65\,\mathrm{m}$, and $C=1.322\times10^3\,\mathrm{N/m^3}$. Note that in this model, the modal damping ratio is not constant for the beam; for example, $\xi_1=0.00253$, $\xi_2=0.000633,\ldots$.

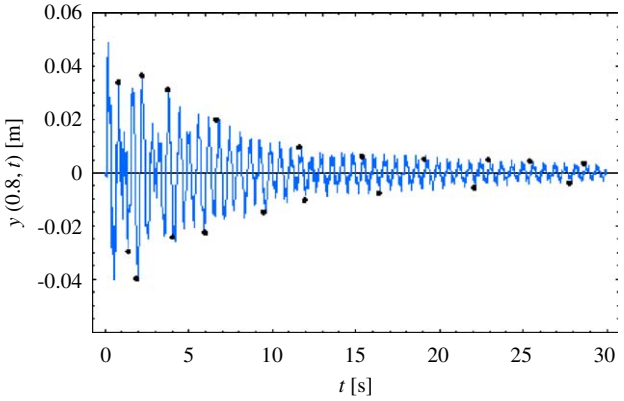

Fig. 2. Comparisons: transient response of the beam at the location $x = 0.8$ m. —: present results and •: Ref. [15].

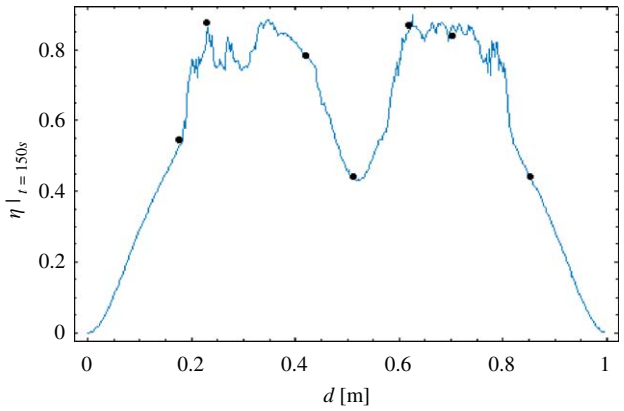

Fig. 3. Comparisons: portion of input energy dissipated by the NES (η) vs. the NES position d. —: present results and •: Ref. [15].

The portion of the input energy dissipated by the viscous damper of the NES (the dynamic damper is also called nonlinear energy sink, see Ref. [15]) at time t_1 is computed by the expression

$$\eta = \frac{E_{\mathrm{NES}}}{E_{\mathrm{in}}} = \frac{\int_0^{t_1} \lambda[\dot{v}(t) - \sum_{r=1}^{n} \dot{a}_r(t)\phi_r(d)]^2 \,\mathrm{d}t}{\int_0^{t_0} F_i[\sum_{r=1}^{n} \dot{a}_r(t)\phi_r(x_F)] \,\mathrm{d}t} \tag{9}$$

where in the case of a moving load, $F_i = F_0$ (see Eq. (6a)) and $x_F = Vt$; in the case of an impulse load (present section), $F_i = F_1$ (see Eqs. (6b) and (8)) and $x_F =$ constant.

E_{NES} is the energy passively absorbed and locally dissipated by the NES, t_1 is assumed to be large enough to assure that the transient dynamics are nearly damped, E_{in} represents the total input energy of the beam due to the load, and $t_0 = T/2$ is the impulse duration.

Figs. 2 and 3 show the comparison between the present model and the results of Ref. [15]; series (4) is truncated at the fifth term and t_1 is set equal to 150 s. Fig. 2 shows $y(0.8, t)$, the response of the beam at $x = 0.8$ m, and Fig. 3 shows the fraction of energy dissipated by the viscous damper, η, for different NES positions. The black dots are reproduced from Ref. [15], and the continuous line represents the present results; good agreement between Ref. [15] and the present model is found.

Fig. 3 shows that for the present problem (fixed location and impulsive excitation), the best position of the dynamic damper is not in the middle, due to broadband excitation and the location of the force.

3.2. Linear dynamic damper and moving load

Further verification of the present model is now carried out, in order to check the accuracy of the approach in the case of moving loads; data from Ref. [4] are used for this purpose.

Consider the system of Fig. 1, with $V(t) =$ constant $\neq 0$ and $f(u) = ku$; the external force has constant amplitude but is moving along the beam, and the dynamic absorber is linear. The external force is given by Eq. (6a).

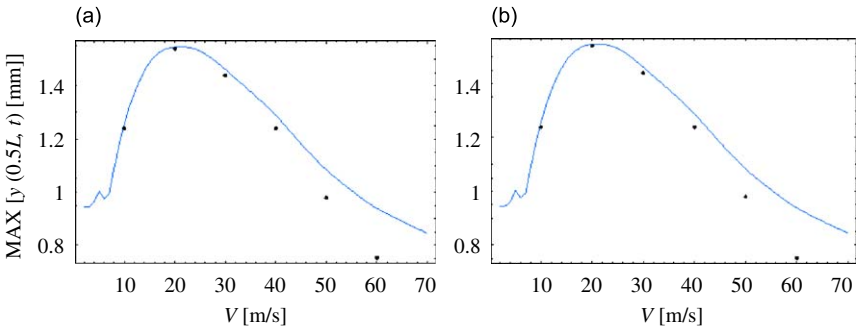

Fig. 4. Comparison of beam subjected to moving load and connected to linear dynamic damper; —: present results and •: Ref. [4]; (a) 1-mode expansion and (b) 5-modes expansion.

For this simulation, the system parameters are: $E = 206\,800$ MPa, $\rho = 7820$ kg/m^3, $A = 0.03$ m $\times$ 0.03 m, $L = 4$ m, $F_0 = 9.8$ N, $\xi_p = 0$ ($p = 1,2,\ldots$) and $m_0 = 1.4076$ kg.

Figs. 4(a) and (b) show the maximum deflection of the mid-span of the beam against the velocity of the moving load. There is a maximum close to $V = 21.5$ m/s, which is 61 percent of the critical velocity as defined in Ref. [1] for moving loads without absorbers. The dynamics are mainly governed by the first mode of the beam, as proven by comparing Figs. 4(a) and (b), where one and five mode expansions are used, respectively. Moreover, good agreement with Ref. [4] is found; the slight differences at high speeds are probably due to the beam modelling. Wu [4] used a finite element method and numerically reduced the governing equations to the first beam mode; here, exact eigenfunctions are used and the reduction of the PDE to ODEs is done analytically. Additionally, different time integration approaches are used.

4. Optimisation of the dynamic damper

In the present section, linear and nonlinear dynamic dampers acting on the beam defined in the previous section (Wu model [4]) are analysed, and different optimisation approaches are applied to find the optimal absorber parameters. When other kinds of beams are analysed, specific data will be given. Two indicators are considered for evaluation of the absorber performance and for optimisation purposes: the maximum vibration amplitude or the factor η (see Eq. (9)).

4.1. Optimisation of the linear dynamic damper

4.1.1. Maximum deflection approach

Consider the system of Fig. 1, with $\xi_p = 0.01$ ($p = 1,2,\ldots$), $V = 21.5$ m/s, and $f(u) = ku$. The optimisation of the dynamic damper is focused on the minimisation of the maximum beam deflection. The stiffness, the viscous damping, and the location of the dynamic absorber can be varied to find the optimum values. It can be proven that the optimal absorber has zero dissipation; in order to avoid numerical problems and improve the time integration efficiency, a very small dissipation of $\lambda = 0.1$ is considered. This means that, for example, in the case of optimal stiffness, the damping ratio of the absorber will be $\xi = 0.001$. The maximum deflection for the undamped bare beam (without dynamic absorber, and with $\xi_p = 0$, $p = 1,2,\ldots$) is 1.6279 mm; for the damped bare beam the maximum deflection is 1.6042 mm. In Figs. 5(a) and (b), the effects of the dynamic damper location and the stiffness on the maximum deflection are presented. Fig. 5(a) is obtained using $k = 1795$ N/m, and Fig. 5(b) results from using $d = 0.55L$ (such stiffness and location are the optimal absorber parameters), and the maximum deflection occurs at $x_{\text{top}} = 0.53L$. It should be noted that the optimal damper location is not sensitive to variation of the other parameters. The maximum transverse deflection, which occurs at $x_{\text{top}} = 0.53L$, is 1.5054 mm (6.15 percent reduction with respect to the bare beam), and the maximum deflection of the middle of the beam is 1.4989 mm.

4.1.2. Energy approach

The second approach is focused on maximisation of the energy dissipated by the dynamic absorber, i.e., the indicator η (see Eq. (9) with $F_i = F_0$ and $x_F = Vt$). The viscous damping and stiffness have been regularly sampled on a 100×100 grid, meaning that the damping resolution is 0.4 N s/m, the stiffness resolution is 20 N/m, and the total number of cases analysed is 10 000. The damper location is $d = 0.55L$, and several numerical tests have proven that this parameter does not greatly change around the middle of the beam. The portion of the input energy absorbed by the dynamic damper η as λ and k are varied is shown in Fig. 6. The maximum, $\eta = 88.9$ percent, is obtained for $\lambda = 10.5$ N s/m and $k = 900$ N/m; the behaviour of η is quite regular, the only maximum is located in a flat region, which assures that the optimum is robust.

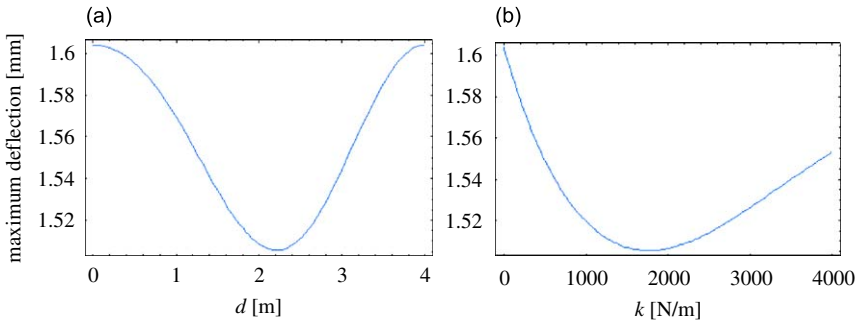

Fig. 5. Optimal location and stiffness of linear dynamic damper for deflection approach: (a) maximum beam deflection vs. damper location ($k = 1795$ N/m) and (b) maximum beam deflection vs. stiffness ($d = 0.55L$).

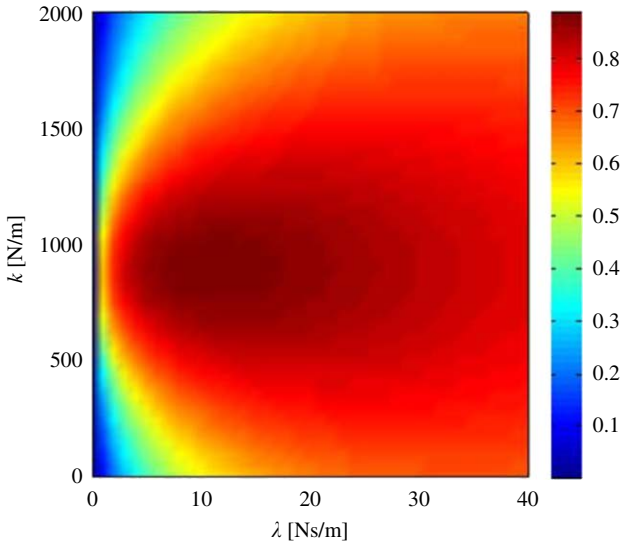

Fig. 6. Linear damper optimisation, energy approach: map of the absorbed energy η.

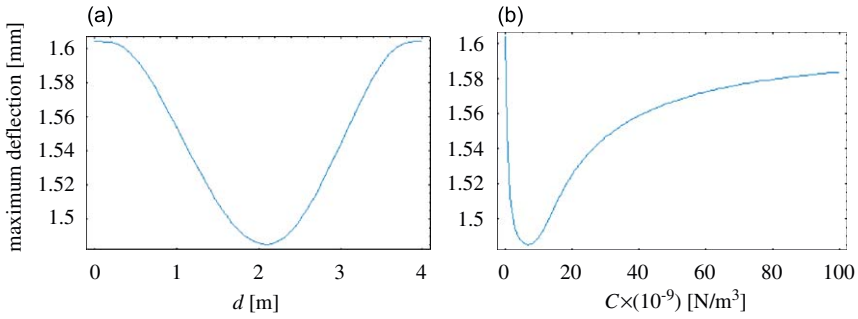

Fig. 7. Optimum location and stiffness of nonlinear absorber for deflection approach: (a) deflection amplitude vs. damper location ($C = 6.7 \times 10^9$ N/m^3) and (b) deflection amplitude vs. stiffness ($d = 0.53L$).

4.2. Optimisation of the nonlinear dynamic damper

4.2.1. Maximum deflection approach

Consider the system of Fig. 1, with $\xi_p = 0.01$ ($p = 1,2,\ldots$), $V = 21.5$ m/s, and $f(u) = Cu^3$. Following the previous section, Figs. 7(a) and (b) show the maximum deflection vs. the damper location and the stiffness, respectively. In Fig. 7(a), $C = 6.7 \times 10^9$ N/m^3 and in Fig. 7(b), $d = 0.53L$. The pair ($C = 6.7 \times 10^9$ N/m^3, $d = 0.53L$) represents the optimal point in the parameter space; the maximum deflection occurs at $x_{\text{top}} = 0.53L$. For the optimal case, the maximum transverse deflection

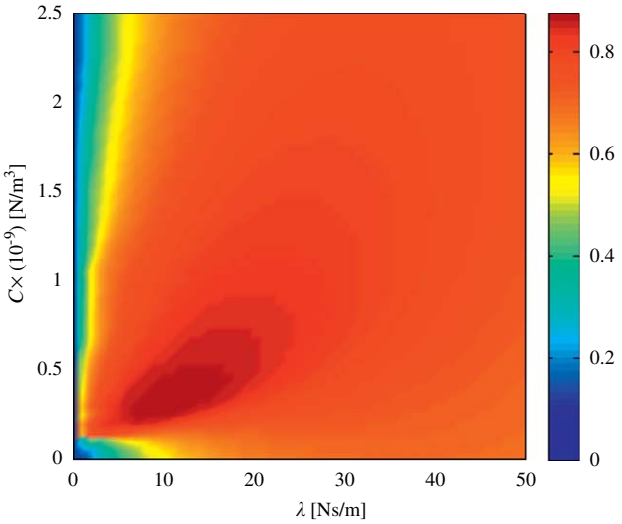

Fig. 8. Optimum η, for nonlinear dynamic damper and energy approach.

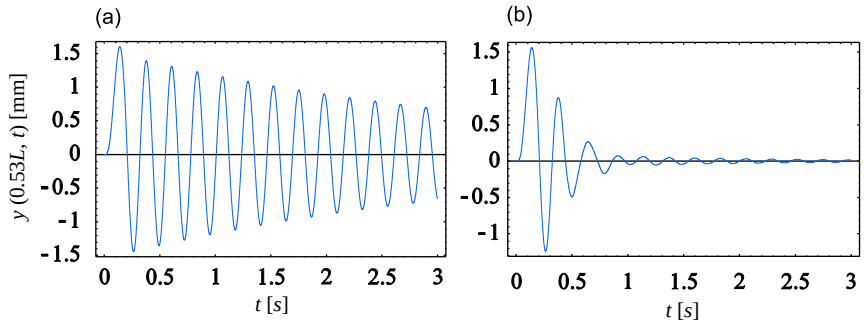

Fig. 9. Transient response of the system: (a) damped beam without dynamic damper and (b) damped beam with nonlinear dynamic damper.

is 1.4852 mm (7.56 percent reduction with respect to bare beam) at this point. The stiffness values of the linear and nonlinear systems are not comparable, as they have different units.

Note that the maximum beam deflection for linear and nonlinear absorbers occurs at $x_{\text{top}} = 0.53L$, but the optimal absorber location in the nonlinear case is closer to the middle ($d = 0.53L$), than in the linear case ($d = 0.55L$). The reduction of the transverse deflection is almost the same for nonlinear absorber locations from $d = 0.51L$ to $0.53L$; for the sake of brevity, details are omitted.

4.2.2. Energy approach

For the approach of maximising the absorbed energy, $d = 0.53L$ is considered, see the considerations of the previous section. The portion of input energy absorbed by the dynamic damper η as λ and C are varied is shown in Fig. 8. The maximum, $\eta = 87.4$ percent, is obtained at $\lambda = 11\,\text{N s/m}$ and $C = 0.30\times10^9\,\text{N/m}^3$. It is interesting to note that, for the case of fixed shock load, the optimal nonlinear dynamic damper absorbs 87 percent of the shock energy of the beam, see Ref. [15]. The parameters are regularly sampled, similarly to Section 4.1. The behaviour of η is regular, as in the linear case, and a unique maximum is found; however, gradients near the optimal point are not small, i.e., it seems less robust than the linear case.

Figs. 9(a) and (b) show the transient response of the system without or with the dynamic absorber, respectively; these figures show the deflection vs. time at the point $x = 0.53L$, near the middle of the beam, where the largest oscillation along the beam occurs. Fig. 9(a) shows the time history for the damped beam without the attachment, and Fig. 9(b) shows the deflection of the same point with the nonlinear dynamic damper attached, and optimised for the maximum absorbed energy ($\lambda = 11\,\text{N s/m}$ and $C = 0.30\times10^9\,\text{N/m}^3$). The effectiveness of the dynamic damper is evident. The number of vibration cycles is strongly reduced with the damper in place, greatly improving the fatigue lifetime.

Table 1 summarises results for the undamped and damped beam, without and with a dynamic damper (linear or nonlinear). For cases 1 and 2 of Table 1, there are no dynamic dampers and the energy cannot be pumped out from the beam, i.e., η must be zero. For cases 3 and 4, there is no beam damping, and the viscous dynamic damper absorbs all of the

Table 1
Comparison between various optimisation results: moving load excitation.

Case	Beam and dynamic damper condition	Stiffness	Viscous damping λ (N s/m)	Dynamic damper location d (m)	Maximum deflection (mm)	Position of maximum deflection (m)	Time of maximum deflection (s)	η (percent)
1	Undamped beam without dynamic damper	0	0	–	1.6279	2.11	0.1398	0
2	Damped beam ($\xi_p = 0.01$) without dynamic damper	0	0	–	1.6042	2.11	0.1401	0
3	Undamped beam with linear dynamic damper, optimal values in Ref. [4]	877.8 N/m	12.98	2	1.6016	2.11	0.1402	99.9
4	Undamped beam with linear dynamic damper, deflection optimisation approach	1795 N/m	0.1	2.2	1.5260	2.12	0.1403	99.6
5	Damped beam with linear dynamic damper, deflection optimisation approach	1795 N/m	0.1	2.2	1.5054	2.12	0.1407	3.4
6	Damped beam with linear dynamic damper, energy optimisation approach	900 N/m	10.5	2.2	1.5306	2.12	0.1401	88.9
7	Damped beam with nonlinear dynamic damper, deflection optimisation approach	6.7×10^9 N/m^3	0.1	2.12	1.4852	2.12	0.1402	2.3
8	Damped beam with nonlinear dynamic damper, energy optimisation approach	0.3×10^9 N/m^3	11	2.12	1.5640	2.12	0.1398	87.4

Table 2
Results for optimisation of the nonlinear dynamic damper with various length.

Beam length L (m)	1	4	10
Velocity at which the max deflection occurs (m/s)	86	21.5	8.6
Dynamic damper mass (kg)	0.3519	1.4076	3.519
Optimised stiffness using the deflection approach, C_{opt} (N/m^3)	$1.7(10^{15})$	$6.7(10^9)$	$1.7(10^6)$
Optimised maximum deflection (mm)	0.0235	1.4852	23.53
Optimised stiffness using the energy approach, C_{opt} (N/m^3)	$80(10^{12})$	$0.30(10^9)$	$80(10^3)$
Optimised viscous damping, λ_{opt} (N s/m)	44	11	4.4
η	87.4%	87.4%	87.4%

energy produced by the external moving load. Therefore, if the time tends to infinity, then η must be 100 percent; accordingly, η is equal to 99.9 and 99.6 percent in cases 3 and 4, respectively. For cases 5 and 7, an extremely low viscous damping of $\lambda = 0.1$ is considered, and absorbs a small portion of energy, 3.4 and 2.3 percent. For cases 6 (linear) and 8 (nonlinear), $\eta = 88.9$ and 87.4 percent, respectively.

For case 3, an undamped beam with linear dynamic damper is considered using optimal values from Ref. [4], and the deflection is reduced only 1.62 percent from the case of the bare beam (case 1). Case 4 (present optimal parameters) shows 6.26 percent deflection reduction. Moreover, case 5, with a damped beam and present optimal parameters, exhibits 6.16 percent deflection reduction from case 2 (damped bare beam). The best deflection reduction, 7.42 percent reduction from case 2, is obtained by using the nonlinear dynamic damper of case 7.

5. Optimisation of the nonlinear dynamic damper: effect of the beam length

In order to understand the effect of the beam length on optimisation of the nonlinear dynamic damper, the following beam lengths are considered: $L = 1$, 4, and 10 m; the other beam parameters are the same as those in Section 3.2 (see also Ref. [4]). The optimal location for the nonlinear dynamic damper remains close to the middle, at $d = 0.53L$. A small viscous damping is considered ($\lambda = 0.1$) when the optimisation of the maximum beam deflection is carried out. The dynamic damper mass remains at 5 percent of the total mass of the structure; this means that the damper mass varies accordingly with the beam length. Results have been reported in Table 2.

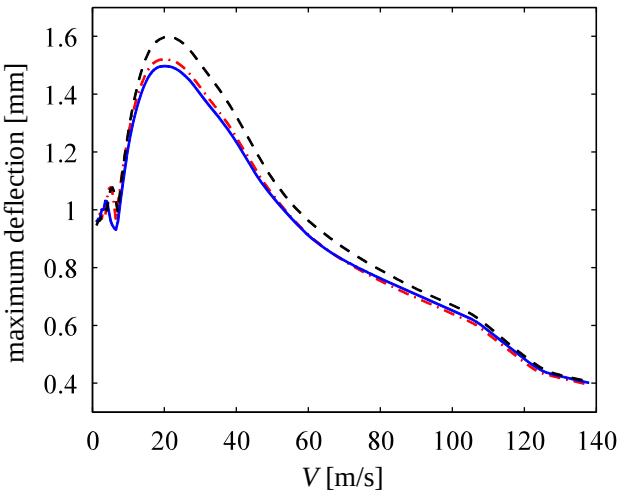

Fig. 10. Maximum deflection vs. the travelling load velocity, effect of dynamic dampers optimised for $V = 21.5$ m/s: - - -: bare beam; - · - · -: linear damper; and ——: nonlinear damper.

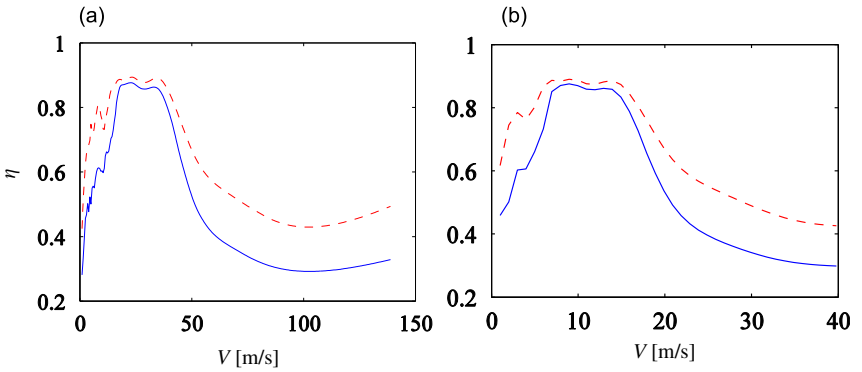

Fig. 11. Portion of input energy absorbed and dissipated by the dynamic damper vs. velocity: (a) $L = 4$ m and (b) $L = 10$ m. - - -: linear dynamic damper and ——: nonlinear dynamic damper.

It is known in the literature that $V_{\text{crit}}L = \text{constant}$, and this result is confirmed; moreover, it is found that $C_{\text{opt}}L^9 = \text{constant}$, for both the maximum deflection and the energy optimisation approaches. For example, when optimising the maximum deflection, $C_{\text{opt}}L^9 = 1.7(10^{15}) \times 1^9 = 6.7(10^9) \times 4^9 = 1.7(10^6) \times 10^9 = 1.7(10^{15})\,\text{N m}^6$; and when optimising the absorbed energy $C_{\text{opt}}L^9 = 80(10^{12}) \times 1^9 = 0.03(10^9) \times 4^9 = 80(10^3) \times 10^9 = 80(10^{12})\,\text{N m}^6$. In each case, $\eta_{\max} = 87.4$ percent and $\lambda_{\text{opt}}L = \text{constant}$ ($\lambda_{\text{opt}}L = 44 \times 1 = 11 \times 4 = 4.4 \times 10 = 44$ Ns). Such conservation laws can be extremely useful for practical designers; indeed, they define classes of structures that exhibit similar behaviour. This means that when the optimal location and stiffness for a particular length are found, they can be straightforwardly extended to other lengths.

6. Effect of the moving load velocity on the dynamic damper performances

Now the behaviour of optimal dynamic dampers is considered over a wide range of moving load velocities. For optimisation of the deflection, the optimal linear and nonlinear stiffness (Table 1), along with $\lambda = 0.1$ N s/m, are used for each case. For the linear dynamic damper, $d = 0.55L$ and $k = 1795$ N/m, and for the nonlinear dynamic damper, $d = 0.53L$ and $C = 6.7 \times 10^9\,\text{N/m}^3$. Fig. 10 shows the maximum deflection vs. the speed of the travelling load. Both linear and nonlinear dynamic dampers allow improved beam behaviour over a wide range of speeds, and the nonlinear dynamic damper is slightly more effective than the linear one in the vicinity of the maximum amplitude ($V = 21.5$ m/s), as can be seen in Fig. 10. At higher speeds, the linear and nonlinear dampers behave in a similar fashion; in either case, the behaviour with dampers is better than that of the bare beam.

In the absorbed energy optimisation approach, the following damper parameters are considered: $\lambda = 10.5$ N s/m and $k = 900$ N/m for the linear dynamic damper, and $\lambda = 11$ N s/m and $C = 0.3 \times 10^9\,\text{N/m}^3$ for the nonlinear damper.

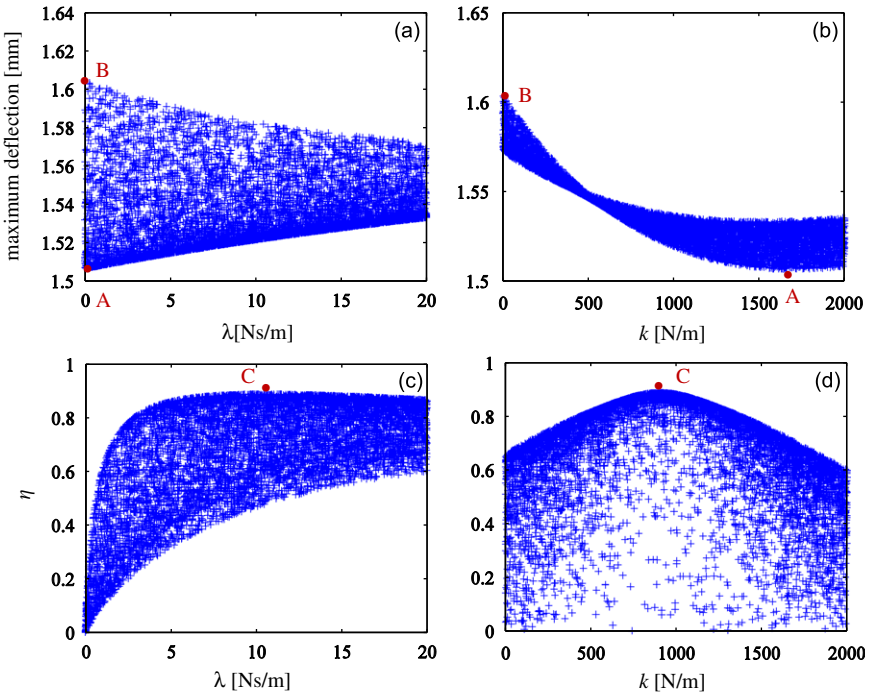

Fig. 12. Random optimisation for linear dynamic damper.

The damper locations are $d = 0.55L$ in the linear case, and $d = 0.53L$ in the nonlinear case. Fig. 11 depicts the fraction of the input energy dissipated by the damper, η, vs. the load velocity for two beam lengths. It is clear that the linear dynamic damper is more effective at absorbing energy than the nonlinear damper; such behaviour seems to be independent of the beam length. These dynamic dampers are more effective around the first critical load velocity; in fact these parameters are optimised at this velocity.

7. Random optimisation

In this section, the optimal parameter set is sought by randomly sampling the parameter space with a uniform distribution. The location of the dynamic damper has a small effect on the two present goal functions (maximum deflection and η), and therefore, only the stiffness and viscous damping are considered in the optimisation process. The total number of cases for the random optimisation is 8000, on the same order as the uniform sampling approach.

For the linear dynamic damper, the optimisation is carried out with the following parameter set ($k \in [0, 2000\,\mathrm{N/m}]$, $\lambda \in [0, 20\,\mathrm{N\,s/m}]$).

Figs. 12(a) and (b) show the effect of the viscous damping and stiffness on the maximum deflection, and Figs. 12(c) and (d) show the effect of the same parameters on η.

Fig. 12 is obtained from the 2-d random search. Since the surface representing the results cannot be easily represented, because of the random distribution of data, a lateral view of this surface is represented. This figure gives some general information about the damper performances; for example, let us consider Fig. 12(a) and $\lambda = 10\,\mathrm{N\,s/m}$; this shows the variation of the maximum deflection as the stiffness k is varied. Even though k cannot be identified from Fig. 12(a) alone, by using Figs. 12(a) and (b), one can easily read the optimal values of λ and k. In Figs. 12(a) and (b), point A indicates the optimum with respect to oscillation amplitude ($k = 1682\,\mathrm{N/m}$, $\lambda = 0.0749\,\mathrm{N\,s/m}$), and the maximum amplitude of oscillation is 1.5055 mm (regular sampling gave 1.5054 mm for $k = 1795\,\mathrm{N/m}$ and $\lambda = 0.1\,\mathrm{N\,s/m}$). Point B shows the maximum deflection of the bare damped beam, $y_{\max} = 1.6042$ mm. In Figs. 12(c) and (d), point C represents the optimum with respect to absorbed energy ($k = 899\,\mathrm{N/m}$, $\lambda = 10.51\,\mathrm{N\,s/m}$), and the energy absorption is 88.9 percent of the input energy (regular sampling gave $\eta = 88.9$ percent for $k = 900\,\mathrm{N/m}$ and $\lambda = 10.5\,\mathrm{N\,s/m}$). By examining Fig. 12(c) near the origin, it can be seen that with $\lambda = 0$, the dynamic damper cannot absorb energy ($\eta = 0$).

The random optimisation obtains results quite close to those found by regular sampling. By using this method, the effect of each parameter becomes clearer in some special situations. For example, Fig. 12(a) shows that high values of the stiffness tend to decrease the effect of viscous damping on the maximum deflection. Fig. 12(b) clearly shows that for $k \approx 500\,\mathrm{N/m}$, the viscous damping has a small effect on the maximum deflection.

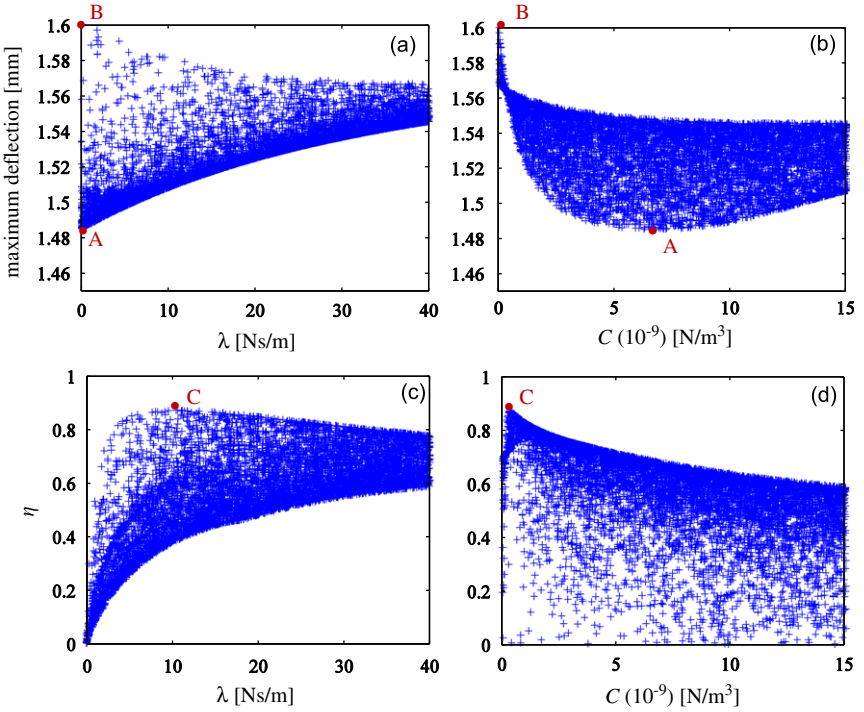

Fig. 13. Random optimisation for nonlinear dynamic damper.

In the case of the nonlinear dynamic damper, the optimisation is carried out with the following parameter set ($C \in [0,\ 15\times10^9\,\mathrm{N/m^3}]$, $\lambda \in [0,\ 40\,\mathrm{N\,s/m}]$). Point A of Figs. 13(a) and (b) indicates the optimum with respect to the maximum deflection ($C = 6.73\times10^9\,\mathrm{N/m^3}$ and $\lambda = 0.0347\,\mathrm{N\,s/m}$); the deflection is $y_{\max} = 1.4850\,\mathrm{mm}$ (in the case of uniform sampling, $y_{\max} = 1.4852\,\mathrm{mm}$, $C = 6.7\times10^9\,\mathrm{N/m^3}$, and $\lambda = 0.1\,\mathrm{N\,s/m}$ were found). Point *B* of Figs. 13(a) and (b) shows the deflection of the bare damped beam, $y_{\max} = 1.6042\,\mathrm{mm}$. Point *C* of Figs. 13(c) and (d) represents the optimum with respect to the absorbed energy. The dynamic damper can absorb up to 87.3 percent of the input energy, with a stiffness of $C = 0.298\times10^9\,\mathrm{N/m^3}$ and $\lambda = 10.60\,\mathrm{N\,s/m}$ (uniform sampling gives $\eta_{\max} = 87.4$ percent, for $C = 0.3\times10^9\,\mathrm{N/m^3}$ and $\lambda = 11\,\mathrm{N\,s/m}$).

8. Conclusions

The performances of linear and nonlinear dynamic absorbers applied to beams excited by moving loads are investigated; the analysis is focused on the transient structural response. Several optimisation strategies are considered, in order to obtain the best set of parameters with respect to the maximum amplitude of vibration or the amount of energy absorbed.

It is confirmed that dynamic dampers are capable of reducing the vibration amplitude in the presence of excitations due to moving loads. Essentially nonlinear (cubic) dynamic dampers are more suitable for reducing the maximum amplitude of vibration, and linear dynamic dampers behave better when the goal is to maximise the vibration energy pumped out from the structure.

The location of the absolute maximum deflection of the beam is near the middle ($x = 0.53L$) for the problems investigated here; the optimal location for the nonlinear damper is at the same location ($d = 0.53L$), and for the linear damper it is at $d = 0.55L$. The maximum fraction of the input energy absorbed by the nonlinear dynamic damper is about 87 percent, regardless of the type of loading or beam geometry.

Using these dynamic dampers can improve the fatigue lifetime of structures. The dynamic absorber causes faster vibration damping, and so the number of cycles decreases, and a moderate reduction of the maximum deflection also greatly increases the fatigue lifetime.

Interesting conservation laws are found for the optimal parameters and beam geometry. The optimal stiffness C_{opt} for reducing the maximum beam vibration and absorbing the vibration energy is related to the beam length, as $C_{\mathrm{opt}}L^9 = \text{constant}$. The optimal damping for maximising the energy pumped out from the structure is related to the beam length by $\lambda_{\mathrm{opt}}L = \text{constant}$. Finally, the optimal damping for reducing the maximum beam vibration is zero. It is

worthwhile to stress that such simple conserved quantities are extremely useful for designers, as they allow generalisation of results to a class of problems.

For the specific problem of a beam under moving loads, there is no real advantage in using essentially nonlinear (cubic) dynamic dampers as opposed to traditional linear dynamic dampers, as the vibration reduction is quite similar. However, the small advantage of the cubic nonlinear damper in reducing the maximum vibration amplitude encourages continued research on other types of nonlinear dampers.

Acknowledgements

The authors would like to thank: Professor Ebrahim Esmailzadeh, Faculty of Engineering and Applied Science, University of Ontario Institute of Technology, for his major constructive comments and the Lab SIMECH/INTERMECH (HIMECH District, Emilia Romagna Region) for supporting the research.

References

[1] L. Frýba, *Vibration of Solids and Structures under Moving Loads*, Telford, London, 1999.
[2] S. Timoshenko, D.H. Young, W. Weaver, *Vibration Problems in Engineering*, fourth ed., Wiley, New York, 1974.
[3] E. Esmailzadeh, M. Ghorashi, Vibration analysis of beams traversed by uniform partially distributed moving mass, *Journal of Sound and Vibration* 184 (1) (1995) 9–17.
[4] J.J. Wu, Study on the inertia effect of helical spring of the absorber on suppressing the dynamic responses of a beam subjected to a moving load, *Journal of Sound and Vibration* 297 (2006) 981–999.
[5] J.P. Den Hartog, *Mechanical Vibrations*, McGraw-Hill, New York, 1985.
[6] A. Greco, A. Santini, Dynamic response of a flexural non-classically damped continuous beam under moving loadings, *Computers and Structures* 80 (2002) 1945–1953.
[7] Y.S. Lee, G. Kerschen, A.F. Vakakis, P.N. Panagopoulos, L.A. Bergman, D.M. McFarland, Complicated dynamics of a linear oscillator with a light, essentially nonlinear attachment, *Physica D* 204 (2005) 41–69.
[8] H.-C. Kwon, M.-C. Kim, I.-W. Lee, Vibration control of bridges under moving loads, *Computers and Structures* 66 (1998) 473–480.
[9] P. Muserosa, M.D. Martinez-Rodrigo, Vibration control of simply supported beams under moving loads using fluid viscous dampers, *Journal of Sound and Vibration* 300 (2007) 292–315.
[10] J.F. Wang, C.C. Lin, B.L. Chen, Vibration suppression for high-speed railway bridges using tuned mass dampers, *International Journal of Solids and Structures* 40 (2003) 465–491.
[11] J.D. Yau, Y.B. Yang, Vibration reduction for cable-stayed bridges travelled by high-speed trains, *Finite Elements in Analysis and Design* 40 (2004) 341–359.
[12] A.K. Das, S.S. Dey, Effects of tuned mass dampers on random response of bridges, *Computers and Structures* 43 (1992) 745–750.
[13] J. Lin, F.L. Lewis, T. Huang, Passive control of the flexible structures subjected to moving vibratory systems, *ASME Special Publication on Active and Passive Control of Mechanical Vibrations, PVP* 289 (1994) 11–18.
[14] J. Lin, Multi-timescale fuzzy controller for a continuum with a moving oscillator, *IEE Proceedings—Control Theory and Applications* 151 (3) (2004) 310–318.
[15] F. Georgiades, A.F. Vakakis, Dynamics of a linear beam with an attached local nonlinear energy sink, *Communications in Nonlinear Science and Numerical Simulation* 12 (2005) 643–651.
[16] A.F. Vakakis, L.I. Manevitch, O. Gendelman, L. Bergman, Dynamics of linear discrete systems connected to local essentially nonlinear attachments, *Journal of Sound and Vibration* 264 (2003) 559–577.
[17] O.V. Gendelman, Targeted energy transfer in systems with non-polynomial nonlinearity, *Journal of Sound and Vibration* 315 (2008) 732–745.
[18] S. Wolfram, *The Mathematica Book, Wolfram Media*, Cambridge University Press, New York, 1996.